SHEP-03-22 LC-TH-2003-063

Associated production of single sneutrino and fermion pairs at polarised photon colliders

Dilip Kumar Ghosh[a,1] and Stefano Moretti [b]

a) Institute of Theoretical Science, Oregon University,

Eugene, OR 97403-5203, USA

b) School of Physics and Astronomy, University of Southampton,

Highfield, Southampton SO17 1BJ, UK

Abstract

We report on single sneutrino production in the context of R-parity-violating Supersymmetry (SUSY) at future $\gamma\gamma$ linear colliders. The sneutrino is produced in association with fermion pairs and it is shown that its decays into two further fermions will lead, in presence of beam polarisation, to a clean signal over the Standard Model (SM) backgrounds.

In this note, we summarise the main results of Ref. [1], where single production of sneutrinos in association with fermion pairs in the R-parity-violating (RPV) Minimal Supersymmetric Standard Model (MSSM) [2] was considered at future polarised photon-photon colliders. The sneutrino is assumed to interact with two fermions via the trilinear L-violating operators (λ_{ijk} and λ'_{ijk}), while preserving B-conservation ($\lambda''_{ijk} = 0$). The channel considered here is in our opinion more suited as a sneutrino 'search' mode in $\gamma\gamma$ collisions than the resonant direct production of Ref. [3], simply because one can scan a wider range of sneutrino masses $M_{\tilde{\nu}}$ (as long as $\sqrt{s_{\gamma\gamma}} \approx 0.8\sqrt{s_{e^+e^-}} \gg M_{\tilde{\nu}}$). This is because in associated production some amount of energy is carried away by the accompanying fermion pair, whereas in direct production the only $M_{\tilde{\nu}}$ attainable is basically the (reduced) CM energy itself. Furthermore, unlike in the case of resonant production, the associate mode may also induce flavour changing final states, so that one has that the corresponding signatures are basically SM background free [4]. Finally, the main advantage of exploiting $\gamma\gamma$ collisions in place of e^+e^- ones [5, 6] in producing single sneutrinos in association with a fermion pair resides in the fact that the cross sections for the former are generally larger than those for the latter. Schematically, one has

$$\gamma\gamma \to \tilde{\nu}\ell^{\pm}\ell'^{\mp} \quad \text{or} \quad \tilde{\nu}q\bar{q}' \quad \text{with} \quad \tilde{\nu} \to \ell''^{\pm}\ell'''^{\mp} \quad \text{or} \quad \tilde{\nu} \to q''\bar{q}''', \tag{1}$$

where the ℓ's refer to e, μ and τ leptons and the q's to d, u, s, c and b quarks.

[1]Talk given at the Extended Joint ECFA/DESY Study on Physics and Detectors for a Linear Electron-Positron Collider, Amsterdam, Netherlands, 1-4 April 2003.

The flavour of the final state fermions will depend upon the RPV couplings involved. In our analysis, we will concentrate on the following L-violating couplings: $\lambda_{311}, \lambda_{323}, \lambda'_{323}$ and λ'_{333}. The reason for selecting this particular set out of the 36 possible couplings is that these are less constrained and at the same time can lead to a significant contribution to the production as well as the decay rates of sneutrinos in (1). Moreover, only one at a time will be allowed to be non-zero.

The dominant decay modes are:

$$\tilde{\nu} \rightarrow f\bar{f}' \quad (f = \ell, q) \quad \text{fermion pairs,} \tag{2}$$

$$\tilde{\nu} \rightarrow \tilde{\chi}_i^0 \nu \quad (i = 1,2,3,4) \;\; \text{neutralino + neutrino,} \tag{3}$$

$$\tilde{\nu} \rightarrow \tilde{\chi}_i^+ \ell^- \quad (i = 1,2) \;\; \text{chargino + lepton.} \tag{4}$$

If the sneutrino is the Lightest SUSY Particle (LSP) LSP, then it will decay through the first (RPV) channel, otherwise via one of the other two (MSSM) modes. In the course of the analysis we assume the Grand Unification (GUT) relationship between the U(1) and SU(2) gaugino mass parameters, $M_1 = \frac{5}{3}\tan^2\theta_W M_2$. Thus, the sneutrino BR into two fermions will depend upon $\mu, M_2, \tan\beta$, $M_{\tilde{\nu}}$ and the magnitude of the RPV coupling. To study the variation of the sneutrino RPV BR we have spanned μ from -500 GeV to $+500$ GeV and M_2 from 100 GeV to 500 GeV.

In Fig. 1(a) we show the contours of constant BR($\tilde{\nu}_\tau \rightarrow e^+e^-$) through the λ_{311} coupling for $M_{\tilde{\nu}_\tau} = 100$ GeV in the $\mu - M_2$ plane, with $\tan\beta = 5$. The region labelled by 'LEP DISALLOWED' is ruled out from the kinematic limit on the lighter chargino mass extracted from LEP-2 data. It can be seen from this figure that the mentioned BR is 90% over a large part of the parameter space. In this case, the lighter chargino is heavier than the sneutrino mass, forbidding the $\tilde{\nu} \rightarrow \tilde{\chi}_1^+\ell^-$ decay channel. The only MSSM channel allowed is $\tilde{\nu} \rightarrow \tilde{\chi}_1^0\nu$, which dominates in the low M_2 region, where $M_{\tilde{\chi}_1^0} < M_{\tilde{\nu}}$. The above scenario changes once the sneutrino becomes heavier, as shown in Fig. 1(b), where the same BR as above is plotted but now with $M_{\tilde{\nu}} = 200$ GeV. In this case, both channels $\tilde{\nu} \rightarrow \tilde{\chi}_1^+\ell^-$ and $\tilde{\nu} \rightarrow \tilde{\chi}_1^0\nu$ make a significant contribution to the total decay width of the sneutrino. (The RPV BR increases with M_2 though, since the lighter chargino and neutralino become heavier.) In Fig. 1(c), this trend becomes very clear: for a 400 GeV sneutrino most of the $\mu - M_2$ plane is covered by the MSSM decays, relegating large RPV BRs to small corners of the parameter space.

This situation changes considerably when the RPV coupling is λ'_{333}. In this case, because of the larger magnitude of the latter, as compared to λ_{311}, the BR($\tilde{\nu} \rightarrow b\bar{b}$) for a 100 GeV sneutrino mass covers almost the entire $\mu - M_2$ plane. Even for heavier sneutrinos (*e.g.*, 200 GeV and 400 GeV), a larger area in the $\mu - M_2$ plane is dominated by the above BR, leaving a smaller region for the MSSM decays than in the previous case: see Figs. 1(d)–(f). Finally, we have noticed that this general behavior of the BRs does not change for higher values of $\tan\beta$. Also, the impact of λ_{323} and λ'_{323} RPV couplings onto the decay rates induces a pattern similar to the one discussed, so we do not reproduce the corresponding figures here.

In Ref. [1], we had performed the numerical analysis for three different points in the MSSM parameter space allowed by LEP-2 data, representing three different natures of the lightest chargino. Here, we only show one case, corresponding to a lightest chargino which is a gaugino dominated state: $\mu = -400$ GeV, $M_2 = 150$ GeV, $\tan\beta = 5$, $M_{\tilde{\chi}_1^0} = 76$ GeV and $M_{\tilde{\chi}_1^\pm} = 150$ GeV.

Furthermore, we select the combinations of incident laser and electron beam polarisations shown in Tab. 1[2].

	$P_{\gamma+}$	$P_{\gamma-}$	P_{e^+}	P_{e^-}
$\sigma(+-)$	$+1$	-1	-0.8	$+0.9$
$\sigma(++)$	$+1$	$+1$	-0.8	-0.9
$\sigma(00)$	0	0	0	0

Table 1: Values of laser and electron(positron) beam polarisations adopted in our analysis. The $\sigma(+-)$ and $\sigma(++)$ denote the polarised production cross-sections, with $\sigma(00)$ the unpolarised one.

To mimic the finite coverage of the LC detectors, we impose the following cuts[3]:

$$\begin{aligned} 5^{\circ} &< \theta < 175^{\circ} \quad \text{(angular cut on both leptons and jets)}, \\ E_\ell &> 5\ \text{GeV} \quad \text{(energy cut on leptons)}, \\ E_j &> 10\ \text{GeV} \quad \text{(energy cut on jets)}. \end{aligned} \tag{5}$$

For illustrative purposes, we assume $\sqrt{s_{e^+e^-}} = 500$ GeV as default. More results at higher energies can be found in [1].

Signals from the λ_{311} coupling

Presence of this coupling leads $\tilde{\nu}_\tau$ to decay into e^+e^- pairs. Hence, the signal corresponding to this L-violating coupling is $e^+e^-e^+e^-$. In Fig. 2(a) we show the variation of $\sigma(\gamma\gamma \to \tilde{\nu}_\tau e^+e^-) *$ BR$(\tilde{\nu}_\tau \to e^+e^-)$ as a function of the $\tilde{\nu}_\tau$ mass. The effect of beam polarisation can be seen very clearly from the figure. At very low sneutrino masses ($<$ 150–200 GeV), $\sigma(++)$, $\sigma(+-)$ and the unpolarised cross-section $\sigma(00)$ are basically the same. As the sneutrino mass rises, the above three cross-sections display a hierarchy, though not dramatic, with $\sigma(+-) > \sigma(00) > \sigma(++)$, whereas, for $M_{\tilde{\nu}_\tau} \geq 0.5\sqrt{s_{e^+e^-}}$, the $\sigma(++)$ component is the one which largely dominates.

[2] Notice that there exists a symmetry amongst the four combinations of laser polarisations, as $(+-)$ and $(-+)$ give the same result, and so do $(++)$ and $(--)$ (see also [7]).

[3] We identify jets with the partons from which they originate.

Signals from the λ_{323} coupling

Presence of this coupling gives rise to the following two types of signals: flavour conserving $\tau^+\tau^-\tau^+\tau^-$ and flavour changing $\mu^+\mu^-\tau^+\tau^-$ (and c.c.'s). The variation of $\sigma(\gamma\gamma \to \tilde{\nu}_\tau \mu^+\tau^-) *$ BR$(\tilde{\nu}_\tau \to \mu^-\tau^+)$ as a function of the sneutrino mass is shown in Figs. 2(b). In this case the final state will have three different combinations of charged particles with identical rates: $\mu^+\mu^-\tau^+\tau^-$, $\mu^+\mu^+\tau^-\tau^-$ and $\mu^-\mu^-\tau^+\tau^+$. Hence, the individual channels will be 1/3 of the total cross-section shown in the figures. The plots for the flavour conserving final state are displayed in Fig. 2(c).

Again, we see that the dominant cross-section comes from $\sigma(++)$ once that $M_{\tilde{\nu}_\tau} \geq 0.5\sqrt{s_{e^+e^-}}$. However, at lower sneutrino masses, the pattern is different from the previous case. The ordering $\sigma(+-) > \sigma(00) > \sigma(++)$ in the intermediate mass regime and the convergence of the rates for all polarisation states at small $M_{\tilde{\nu}_\tau}$ values hold only for $\tau^+\tau^-\tau^+\tau^-$, not for $\mu^+\mu^-\tau^+\tau^-$ (plus c.c.s), for which the unpolarised cross sections are always largest.

Signals from the λ'_{323} coupling

Presence of this coupling gives rise to the following three types of signals: the flavour conserving $s\bar{s}s\bar{s}$ and $b\bar{b}b\bar{b}$ plus the flavour changing $s\bar{s}b\bar{b}$ (and c.c.'s). The variation of $\sigma(\gamma\gamma \to \tilde{\nu}_\tau b\bar{s}) *BR(\tilde{\nu}_\tau \to \bar{b}s)$ as a function of the sneutrino mass is shown in Fig. 2(e). Notice that in this case too there are three equiprobable signatures: $ss\bar{b}\bar{b}$, $s\bar{s}b\bar{b}$ and $\bar{s}\bar{s}bb$. Corresponding plot for the flavour conserving modes are displayed in Fig. 2(d).

The dependence upon the beam polarisation configuration is basically the same as the one described in the previous section, once one establishes a correspondence between the identical- and different-flavour final states in the two cases.

Signals from the λ'_{333} coupling

Presence of this coupling will also give rise to the signal $b\bar{b}b\bar{b}$. The numerical results for the corresponding production cross-sections are shown in Figs. 2(f).

As for the beam polarisation dependence, here, one can see the usual dominance of $\sigma(++)$ whenever $M_{\tilde{\nu}_\tau} \geq 0.5\sqrt{s_{e^+e^-}}$, with the $\sigma(+-)$ component dominating in the intermediate regime. For lower masses, the energy dependence is such that at 500 GeV $\sigma(+-)$ is above $\sigma(00)$.

The SM irreducible background

A variety of SM sub-processes could produce sizable irreducible backgrounds, although at very heavy $M_{\tilde{\nu}}$ values only the tails of the SM distributions can actually play a role. All these channels can be conveniently grouped into general four-fermion final states, of the type $e^+e^-e^+e^-$, $\mu^+\mu^-\tau^+\tau^-$, $\tau^+\tau^-\tau^+\tau^-$, $s\bar{s}s\bar{s}$, $s\bar{s}b\bar{b}$ and $b\bar{b}b\bar{b}$.

	$e^+e^-e^+e^-$	$\mu^+\mu^-\tau^+\tau^{-*}$	$\tau^+\tau^-\tau^+\tau^-$	$s\bar{s}s\bar{s}$	$s\bar{s}b\bar{b}^*$	$b\bar{b}b\bar{b}$
$\sigma(+-)$	4.7×10^9	2169	232	532048	3409	313
$\sigma(++)$	4.7×10^9	2288	233	551620	3485	317
$\sigma(00)$	4.7×10^9	2228	232	541824	3447	315
$\sqrt{s_{e^+e^-}} = 500$ GeV						
*Other c.c.'s are free from SM background						

Table 2: Cross sections in femtobarns for the full four-fermion SM processes discussed in the text, for the three beam polarisation configurations in Tab. 1, after the cuts in (5) (and $M_{e^+e^-} > 1$ GeV for the $e^+e^-e^+e^-$ final state). Notice that no summation over u, d and s (light) flavours has been performed in the case of signatures involving s quarks.

$M_{\tilde{\nu}}$ (GeV)	$e^+e^-e^+e^-$	$\mu^+\mu^-\tau^+\tau^{-*}$	$\tau^+\tau^-\tau^+\tau^-$	$s\bar{s}s\bar{s}$	$s\bar{s}b\bar{b}^*$	$b\bar{b}b\bar{b}$
100	0.1908	0.4650	0.2565	2.387	2.100	1.3091
	382042836	56	19	93366	627	63
200	0.00234	0.00695	0.00313	0.3870	0.4019	0.17967
	93921298	6.4	4.4	22248	170	18
300	0.000171	0.000493	0.000222	0.04387	0.0477	0.01649
	19052146	3.6	1.7	3696	30	3.3
*Other c.c.'s are free from SM background						

Table 3: Cross sections in femtobarns for the four-fermion final states discussed in the text, for both signals (first row) and backgrounds (last row), for unpolarised beams at $\sqrt{s_{e^+e^-}} = 500$ GeV , after the cuts in (5) plus the additional constraint $|M_{ff} - M_{\tilde{\nu}}| < 5$ GeV, for several sneutrino masses. (Here, ff refer to either lepton-lepton or jet-jet pairs and only one $M_{\tilde{\nu}}$ is required to be reconstructed.) Notice that, for the backgrounds, no summation over u, d and s (light) flavours has been performed in the case of signatures involving s quarks.

The first three signatures only receive EW contributions (*i.e.*, they are of $\mathcal{O}(\alpha^4)$), whereas the last three also have a QCD induced component of $\mathcal{O}(\alpha^2\alpha_s^2)$. Under the assumption of perfect b (and c) quark tagging, we only need to sum over light quark flavours in the case of $s\bar{s}s\bar{s}$ and $s\bar{s}b\bar{b}$ final states, not of $b\bar{b}b\bar{b}$. However, in order to save computing time, we have presently refrained from doing so, as the EW and QCD contributions involving only s (anti)quarks, as opposed to the sum over u, d and s, already swamp the signal in the accessible $M_{\tilde{\nu}}$ regions. (All forthcoming $s\bar{s}s\bar{s}$ and $s\bar{s}b\bar{b}$ background rates will then be reported for s flavours only.)[4]

[4]We have used the two-loop expression for α_s, as a function of $Q \equiv \sqrt{s_{\gamma\gamma}}$ and of $\Lambda^{n_f=4}_{\rm QCD} = 0.230$ GeV.

$M_{\tilde{\nu}}$ (GeV)	$e^+e^-e^+e^-$	$\mu^+\mu^-\tau^+\tau^-$	$\tau^+\tau^-\tau^+\tau^-$	$s\bar{s}s\bar{s}$	$s\bar{s}b\bar{b}$	$b\bar{b}b\bar{b}$
100	0.00031	2.0	1.9	0.25	2.7	5.2
200	7.6 $\times 10^{-6}$	0.087	0.047	0.082	0.97	1.3
300	1.2 $\times 10^{-6}$	0.0082	0.0054	0.023	0.28	0.29

Table 4: Significances $S/\sqrt{B}$ at $\sqrt{s_{e^+e^-}} = 500$ GeV after 1 ab^{-1} for the four-fermion final states discussed in the text, for both signals (first row) and backgrounds (last row), for unpolarised beams, after the cuts in (5) plus the additional constraint $|M_{ff} - M_{\tilde{\nu}}| < 5$ GeV, for several sneutrino masses. (Here, ff refer to either lepton-lepton or jet-jet pairs and only one $M_{\tilde{\nu}}$ is required to be reconstructed.) Notice that, for the backgrounds, no summation over u, d and s (light) flavours has been performed in the case of signatures involving s quarks.

The SM background cross-sections, after the cuts listed in eq. (5), are given in Tab. 2. A common feature to all rates is that they are basically independent of the polarisation state of the initial particles[5]. By comparing the background rates in Tab. 2 to those for the signals in Fig. 2, it is clear that the former are overwhelming the latter in the *inclusive* cross sections. However, several selection cuts can be applied in order to improve the signal-to-background ratio (S/B). For example, the Z mediated noise in four-lepton final states can be reduced by requiring that no $\ell^+\ell^-$ pairs of opposite charge (with $\ell = e, \mu$) reproduces the Z mass within a few GeV (say, 3 or 4, given the good mass resolution expected at LCs for electrons and muons). Similarly, one can proceed for four-quark final states, by rejecting events with one (or more) jet-jet invariant masses in the vicinity of the Z and $W^\pm$ peaks. The 4τ signature is more difficult to deal with in this respect, because of the missing momentum carried away by the neutrinos. Finally, QCD induced four-jet backgrounds tend to produce at least one jet-jet pair with small invariant mass.

In the very end, however, one should keep in mind that we are dealing with sneutrino masses that are bound by current experimental constraints to be above the EW scale. Hence, in general, by restricting oneself to the most interesting mass range, sufficiently far from the Z and $W^\pm$ masses, say, 100–150 GeV or above, the chances of extracting the RPV signals in some of the channels discussed become evident, if one refers to Fig. 3 and to the rates in Fig. 2.

By finally recalling that sneutrinos yield mass resonances that are rather narrow (see the typical widths in the Appendix of Ref. [1]), one can further enhance the S/B by restricting the candidate sample around the resonances. To this end, we present Tab. 3, where, alongside the

[5]The huge rates for the $e^+e^-e^+e^-$ final state should not be surprising: on the one hand, because of the t, u channel soft and collinear singularities of the total cross section (which are only regulated by the small electron mass); on the other hand, since we have implemented rather loose constraints in order to avoid these, *i.e.*, other than the cuts in individual energy and polar angles of eq. (5) we only required $M_{e^+e^-} > 1$ GeV on all electron-positron pairs (this combination is sufficient to obtain a numerically stable answer).

signal yield, the surviving background rates are given, after we have required that only one (di-lepton or di-jet) invariant mass reconstructs the resonant sneutrino mass within 10 GeV. Notice that we have accounted for all combinatorics in both leptonic and hadronic final states, assuming EM charge recognition in the former but not in the latter. Results are given for the unpolarised case, for the sake of illustration. (In the case of polarised initial states, the pattern is very similar.)

At the end of this selection, one should expect the final states $\mu^+\mu^-\tau^+\tau^-$, $\tau^+\tau^-\tau^+\tau^-$ and $b\bar{b}b\bar{b}$ to achieve sizable significances $\sigma \equiv S/\sqrt{B}$ after 1 ab^{-1} of luminosity in the region $M_{\tilde{\nu}} \sim 100$–150 GeV, larger than 5 in the case of the hadronic signature and limitedly to ≈ 2 for the leptonic ones. The overall signal rates at that luminosity are about 1,000 events per channel. All other signatures appear instead hopeless. The typical signal would then be an excess of $\mu^+\mu^-\tau^+\tau^-$, $\tau^+\tau^-\tau^+\tau^-$ plus $b\bar{b}b\bar{b}$ events above the SM expectations for the corresponding four-fermion processes, with the bulk of the events cantered in a rather narrow lepton-lepton or jet-jet mass region corresponding to the sneutrino mass.

In summary, if RPV couplings of the type λ_{311}, λ_{323}, λ'_{323} or λ'_{333} are close to their current exclusion bounds, over sizable regions of the MSSM parameter space (particularly, for positive μ values), several four-fermion signatures induced by a sneutrino, with a mass $M_{\tilde{\nu}} \lesssim 150$ GeV if $\sqrt{s_{e^+e^-}} = 500$ GeV[6], produced in association with a fermion pair and decaying itself into a second pair, can be accessed in $\gamma\gamma$ collisions with the photons produced via laser light back-scattering against the primary electrons and positrons. The typical annual rate should be of several hundreds to a thousand events in each of the three channels $\mu^+\mu^-\tau^+\tau^-$, $\tau^+\tau^-\tau^+\tau^-$ and $b\bar{b}b\bar{b}$, depending on the actual sneutrino mass and assuming a luminosity of 1 ab^{-1}.

Furthermore, since typical SM backgrounds have been seen to be less sensitive than the signals to the polarisation state of the incoming particles, one may exploit the latter in order to improve the discovery potential of RPV signals at future LCs. If a high, but not unrealistic, degree of polarisation of both laser photons and leptonic beams can be achieved, this can be exploited to push the discovery reach in sneutrino mass somewhat beyond the mentioned $M_{\tilde{\nu}}$ values in the $\tau^+\tau^-\tau^+\tau^-$ and $b\bar{b}b\bar{b}$ final states (*i.e.*, those most massive in the leptonic and hadronic case, respectively). At 500 GeV, the polarisation combination in which the electron and positron helicities have the opposite sign and are also opposite to those of the corresponding laser photons yields, for sneutrino masses in the 100–250 GeV region, signal rates somewhat higher than those induced in the other cases (including that of unpolarised beams), up to a factor of 2. In contrast, for the $\mu^+\mu^-\tau^+\tau^-$ final state, it is the unpolarised configuration the most suitable for sneutrino searches in the above mass range[7]. The polarisation state in which the electron and positron helicities have the same sign and opposite to the one of the laser photons would turn out extremely

[6]For $\sqrt{s_{e^+e^-}} = 1$ TeV, the limit becomes $M_{\tilde{\nu}} \lesssim 250$ GeV [1].

[7]Once the collider energy is raised to 1 TeV, differences between the three polarisation combinations almost disappear if $M_{\tilde{\nu}} \lesssim 250$ GeV [1].

useful for heavier sneutrino masses, as signal rates are here consistently and significantly above those induced by the other polarisations, up to a factor of 4 in some instances. Unfortunately, this mass interval is unattainable through present LC designs (TESLA, NLC and JLC) and will have to attend for higher collider energies, such as those foreseen for CLIC ($\sqrt{s}_{e^+e^-} \gtrsim 3$ TeV).

Finally, recall that, as a bonus of the production process considered here, some leptonic signatures which are flavour changing, such as $\mu^+\mu^+\tau^-\tau^-$ and $\mu^-\mu^-\tau^+\tau^+$, would come practically free from SM background, hence promptly detectable at any future LC.

References

[1] D.K. Ghosh and S. Moretti, Phys. Rev. D **66**, 035004 (2002).

[2] L.J. Hall and M. Suzuki, *Nucl. Phys.* **B231**, 419 (1984); R. Barbieri and A. Masiero, *Nucl. Phys.* **B267**, 679 (1986); S. Dimopoulos and L.J. Hall, *Phys. Lett.* **B207**, 210 (1988); V. Barger, G. F. Giudice and T. Han, *Phys. Rev.* D **40**, 2987 (1989); M. Czakon and J. Gluza, hep-ph/0003228; R. Godbole, P. Roy and X. Tata, *Nucl. Phys.* **B401**, 67 (1993); G. Bhattacharyya, J.R. Ellis and K. Sridhar, *Mod. Phys. Lett.* **A10**, 1583 (1995); G. Bhattacharyya, D. Choudhury and K. Sridhar, *Phys. Lett.* **B355**, 193 (1995); D. Choudhury and S. Raychaudhury, *Phys. Lett.* **B401**, 54 (1997); D.K. Ghosh, S. Raychaudhuri and K. Sridhar, *Phys. Lett.* **B396**, 177 (1997); K. Huitu, J. Maalampi, M. Raidal and A. Santamaria, *Phys. Lett.* **B430**, 355 (1998); G. Moreau, '*Phenomenological study of the interactions violating the R-parity symmetry in the supersymmetric theories*', Ph.D. Thesis, hep-ph/0012156 and references therein.

[3] S. Bar-Shalom, G. Eilam, J. Wudka and A. Soni, *Phys. Rev.* D **59**, 035010 (1999).

[4] M. Chaichian, K. Huitu, S. Roy and Z.H. Yu, *Phys. Lett.* **B518**, 261 (2001).

[5] S. Dimopoulos and L.J. Hall, in [2]; M. Czakon and J. Gluza, in [2].

[6] V. Barger, G. F. Giudice and T. Han, in [2].

[7] S. Berge, M. Klasen and Y. Umeda, *Phys. Rev.* D **63**, 35003 (2001);

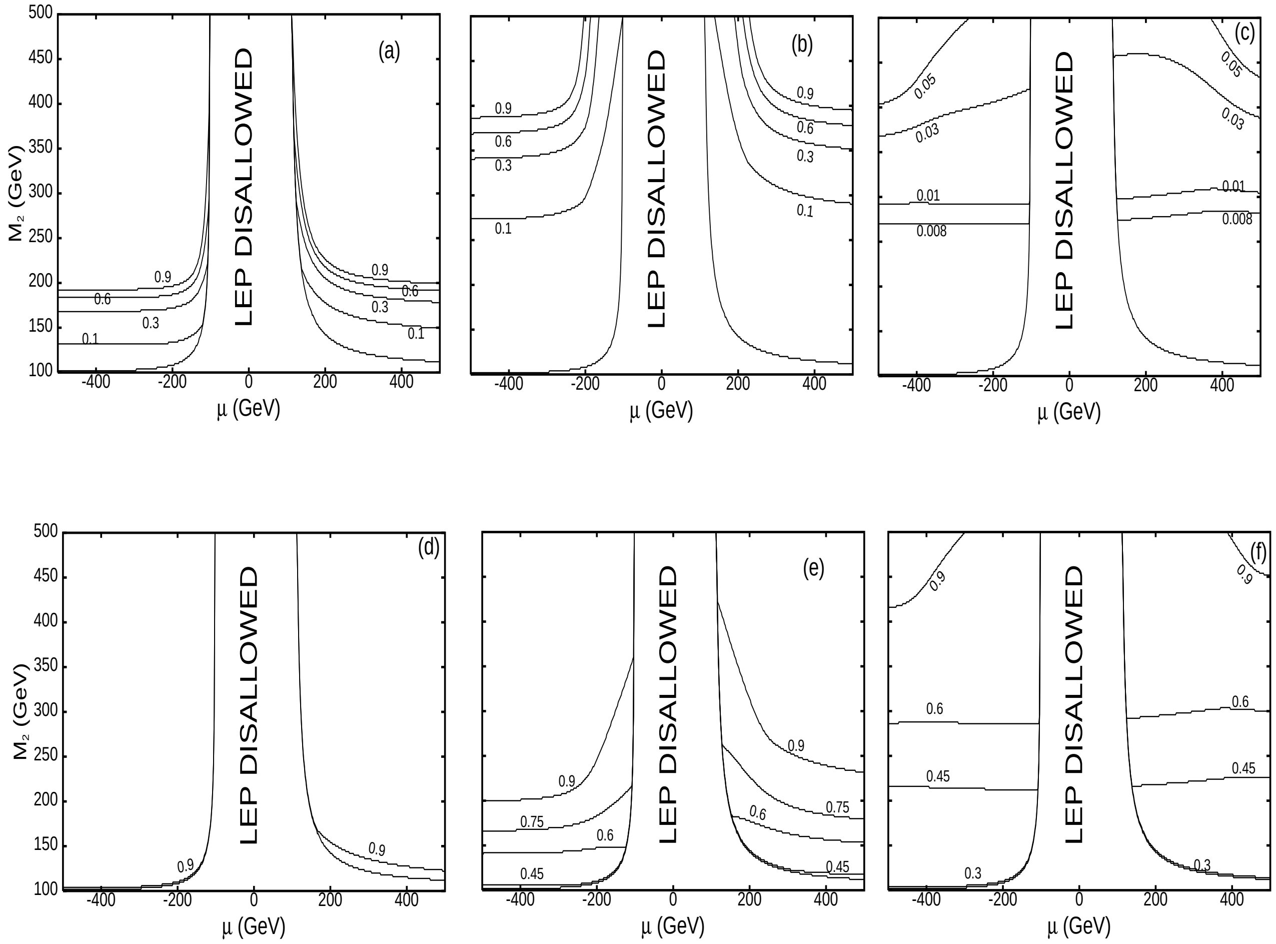

Figure 1: Constant BR contours of the decay $\tilde{\nu}_\tau \to e^+e^-$ for three values of sneutrino masses: 100 GeV (a), 200 GeV (b) and 400 GeV (c). Figs. (d)–(f) represents contours of constant BR$(\tilde{\nu}_\tau \to b\bar{b})$, again for a 100, 200 and 400 GeV sneutrino mass, respectively. The relevant L-violating couplings are here: $\lambda_{311} = 0.062$ for (a)–(c) and $\lambda'_{333} = 0.45$ for (d)–(f). The level curves are function of μ and M_2.

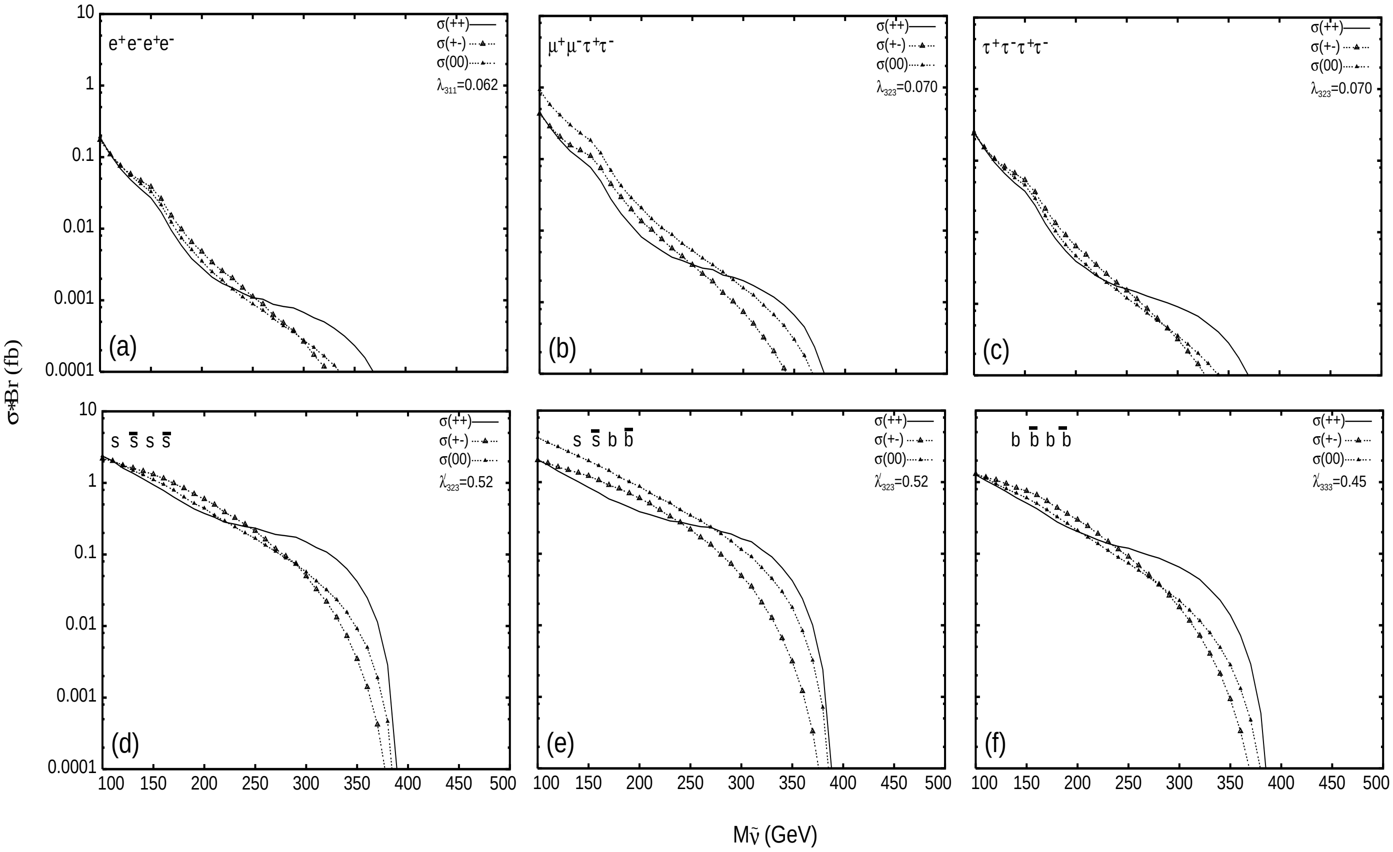

Figure 2: Variation of $\sigma(\gamma\gamma \to \tilde{\nu}_i f_j \bar{f}_k) * \mathrm{BR}(\tilde{\nu}_i \to f_j \bar{f}_k)$ at $\sqrt{s_{e^+e^-}} = 500$ GeV with the sneutrino mass, for fixed values of the relevant λ_{ijk} and λ'_{ijk} couplings. The MSSM parameters are $\mu = -400$ GeV, $M_2 =$ 150 GeV and $\tan\beta = 5$. Final state fermions are shown in the respective figures. For dissimilar fermions in the final state we include all charge conjugate states. See Tab. 3 for the definition of (un)polarised cross-sections.

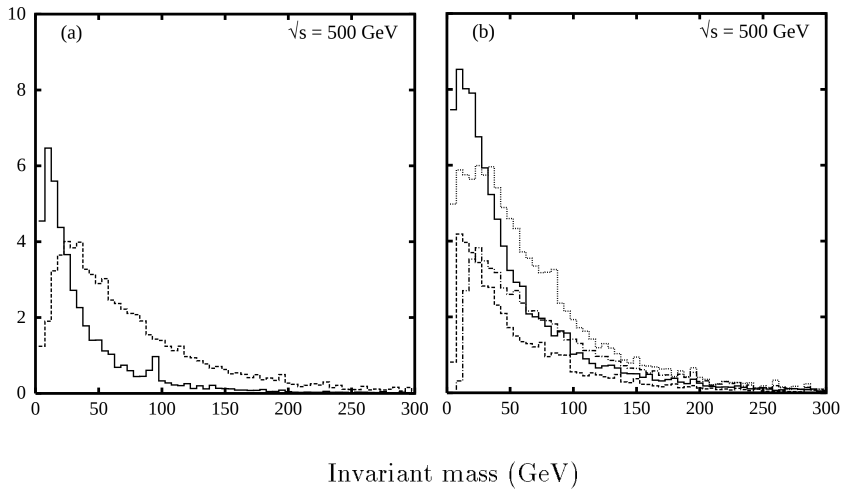

Figure 3: Invariant mass distributions in lepton-lepton and jet-jet pairs reproducing the sneutrino mass in the background processes discussed in the text, for the case of unpolarised beams, after the cuts in (5) (the additional constraint $M_{e^+e^-} > 1$ GeV has been implemented for the $e^+e^-e^+e^-$ signature, for all possible pairings with opposite EM charge). All possible combinatorial combinations have been plotted, each with the same probability, given by the event weight divided by the number of possible pairings in each case. Bins are 10 GeV wide. Normalisation is arbitrary.